

# Brillouin Spectroscopy Reveals Mechanical Properties Beyond Hydration

Zhe Wang,<sup>1</sup> Maria Regato Herbella,<sup>1</sup> Fereydoon Taheri,<sup>1</sup> Maria de los Angeles De la Cruz Garcia,<sup>1</sup> Gaurav Dave,<sup>1</sup> and Christine Selhuber-Unkel<sup>1†</sup>

<sup>1</sup> Institute for Molecular Systems Engineering and Advanced Materials (IMSEAM), INF 225, Heidelberg University, 69120, Heidelberg, Germany.

\*Contact author: pam@inst.org

†Contact author: mmm@inst.org

**ABSTRACT.** Characterizing the micromechanical properties of cells and extracellular matrices is critical in mechanobiology. To meet this need, Brillouin light scattering (BLS) has emerged as a noncontact, high-resolution elastography tool that probes the GHz-frequency longitudinal modulus of materials. This longitudinal modulus reflects both elastic and viscous behavior at microscopic scales. However, interpreting Brillouin spectra in biological specimens is challenging: in highly hydrated samples the Brillouin shift is dominated by water dynamics, and the GHz longitudinal modulus does not directly equate to conventional low-frequency stiffness measures (e.g. Young's or shear moduli). Debates remain about how hydration and polymer relaxation influence the Brillouin signal, and how to relate it to macroscopic biomechanics. In particular, the longitudinal viscosity measured by Brillouin scattering includes a contribution from bulk viscosity, which is absent in standard shear rheology and often overlooked. To address these issues, we used different hydrogel systems and solvent mixtures to show Brillouin spectra are modulated but not dominated by hydration. By varying gelatin concentration, we demonstrated that Brillouin shifts can either positively or negatively correlate with water content, depending on the underlying mechanical response. Measurements on ethanol–water mixtures further clarify this behavior. Although the Brillouin shift varies strongly with composition, it does not follow water content monotonically and instead reflects changes in the mixture's mechanical properties. By comparing longitudinal, bulk, and shear viscosities, we also showed that bulk viscous dissipation plays a significant role in the Brillouin response. These results established a mechanical framework for interpreting Brillouin spectrum in hydrated and biomolecular systems.

## I. INTRODUCTION

Mechanical properties are not only critical to the physiological function of living cells and tissues but also essential to regulate at the cellular level [1]. These properties arise from several factors, including the cytoskeleton, the extracellular collagen-elastin network, and cellular water content [2]. While classical mechanical methods, such as AFM, rheometer and nano indenter, have provided fundamental insights, often lack the spatial resolution to probe micromechanical properties at subcellular scales. Thus, Brillouin light scattering (BLS) has emerged as a promising optical technique to address this gap, offering non-invasive measurements of viscoelasticity through interactions with acoustic phonons [3-6]. As an all-optical confocal system, Brillouin microscope (BM) is uniquely capable of detecting internal mechanical properties in living cells [7,8]. In fact, numerous studies demonstrate that BM serves as a novel mechanical analysis method, providing unique contrast for imaging living cells, organisms, tissue sections, and the cornea [8-11].

For this reason, increasing attention has been paid in recent years to the interpretation of Brillouin scattering frequencies. This interest has prompted debate over whether the high-frequency longitudinal moduli measured by BM can be directly applied in biological and medical contexts as a replacement for low-frequency mechanical characterization such as AFM and rheometer. For example, it has been shown that Brillouin frequencies cannot reliably distinguish the mechanical properties of different molecular weight of polyethylene oxide (PEO) with same water content [12]. It seems that local mechanical properties of cells and tissues measured by Brillouin spectroscopy are primarily determined by their water content [13]. By contrast, other studies report that, over a wider range

\*Contact author: pam@inst.org

†Contact author: mmm@inst.org

of water concentrations, Brillouin frequencies in hydrogels exhibit strong correlations with results from traditional mechanical testing [14]. In addition, correlations between shear and longitudinal moduli have also been observed in several biological systems [15].

Therefore, a deeper understanding of BM measurement and their biological significance is essential. In this work, we investigate the mechanical and Brillouin responses of hydrogels with systematically varied water content to clarify the physical origin and interpretation of Brillouin measurements. We explained the linear correlation between Brillouin frequency shift and water content in certain systems. In addition, a second type of hydrogel exhibits markedly different mechanical responses as a function of water content due to changes in crosslinking. This behavior demonstrates that BM probes intrinsic mechanical properties rather than an extraneous parameter. Variations in water content therefore act as a driver of mechanical changes, not as the quantity directly measured by Brillouin scattering.

Finally, we would like to emphasize the physical significance of the Brillouin frequency linewidth. In current biological applications, attention was typically focused on the Brillouin frequency shift, while the linewidth was often overlooked. Here, we used a simple solution system to elucidate its physical meaning. Furthermore, our results demonstrated that it is far from negligible in most liquids and can even exceed the shear viscosity.

## II. Theoretical background

Brillouin scattering is the inelastic scattering of light by thermally driven density fluctuations propagating at the sound velocity of the medium. The resulting

Brillouin frequency shift  $v_B$  is directly related to the speed of sound  $u$  in the material and the angle of the scattered light  $\theta$ , which is

$$v_B = \frac{2n}{\lambda} u \sin\left(\frac{\theta}{2}\right), \quad (1)$$

where  $n$  is the refractive index,  $\lambda$  is the wavelength [6]. The longitudinal storage modulus  $M'$  is related to the acoustic velocity through

$$M' = \rho u^2 = \rho \left(v_B \frac{\lambda}{2n \sin(\theta/2)}\right)^2, \quad (2)$$

where  $\rho$  is the density. The corresponding longitudinal loss modulus  $M''$  is related to the linewidth (full width at half maximum)  $\Gamma_B$  according to [14]:

$$M'' = \rho v_B \Gamma_B \frac{\lambda^2}{2n \sin(\theta/2)}. \quad (3)$$

The longitudinal viscosity then can be estimated by [16,17]:

$$\eta_{\text{long}} = \frac{M''}{\omega_B} = \frac{\rho \Gamma_B}{8\pi} \frac{\lambda^2}{n \sin(\theta/2)}. \quad (4)$$

For Newtonian liquids, the viscosity is independent of frequency, so the viscosity measured by BM should agree with that in low frequency. However, it is also important to note that longitudinal viscosity and shear viscosity are not equal. To understand the distinction, we consider the Navier-Stokes equation for incompressible Newtonian fluids:

$$\rho \left[ \frac{\partial \mathbf{u}}{\partial t} + (\mathbf{u} \cdot \nabla) \mathbf{u} \right] = -\nabla P + \eta_s \Delta \mathbf{u}, \quad (5)$$

where  $P$  is the pressure and  $\eta_s$  is the shear viscosity. This equation expresses Newton's second law for a viscous fluid, describing the motion of a liquid under applied forces. The last term represents viscous stress. In this form, the liquid is assumed to be incompressible, which is appropriate for low-frequency shear rheology where,

$$\nabla \cdot \mathbf{u} = 0. \quad (6)$$

But this is not the case especially for high frequency. For a compressible Newtonian liquid, the Navier-Stokes equation can be written as [18]

$$\begin{aligned} \rho \left[ \frac{\partial \mathbf{u}}{\partial t} + (\mathbf{u} \cdot \nabla) \mathbf{u} \right] \\ = -\nabla P + \eta_s \Delta \mathbf{u} + \left( \eta_b + \frac{4}{3} \eta_s \right) \nabla (\nabla \cdot \mathbf{u}). \end{aligned} \quad (7)$$

The last term represents a viscous force that resists spatially non-uniform compression or expansion of the fluid, arising when different regions change volume at different rates. This contribution involves two viscosity coefficients. One is the familiar shear viscosity  $\eta_s$  and the other one is bulk viscosity  $\eta_b$ , also known as second viscosity, volume viscosity or

expansion coefficient of viscosity [19-21]. In liquids and gases, molecules possess translational, rotational, and vibrational degrees of freedom. The shear viscosity  $\eta_s$  is associated primarily with translational motion. In contrast, the bulk viscosity  $\eta_b$  arises from the relaxation of rotational and vibrational degrees of freedom. These effects combine to define the longitudinal viscosity, which equals the sum of the bulk viscosity and four-thirds of the shear viscosity, as shown below:

$$\eta_{\text{long}} = \eta_b + \frac{4}{3} \eta_s. \quad (8)$$

Within the present Newtonian framework, the viscosity is frequency independent. This addresses the common argument that Brillouin scattering probes only the high-frequency mechanical response rather than low-frequency material properties.

### III. MATERIALS AND METHODS

#### A. Hydrogel preparation

Gelatin from porcine skin type A powder (G1820), 2-Hydroxyethyl methacrylate 99% (477028), Methacrylic acid 99% (155721), Tri(ethylene glycol) dimethacrylate 95% (261548) and, 2-Hydroxy-2-methylpropiophenone 97% (Darocur, 405655) were purchased from Sigma-Aldrich and used as received.

#### 1. Synthesis of Gelatin hydrogels

The Gelatin hydrogels with different gelatin proportion (180, 160, 140, 120, 100, 80, 60 and 40 mg/mL) were prepared dissolving the gelatin powder in 2 mL of distilled water at 60 °C for 1 h. The warm solutions were poured into bottom-glass petri dish and left at 40 °C for 2 h, covering them with parafilm to avoid the loss of solvent. Then the samples were placed at room temperature for 24 h before performing further characterization.

#### 2. Synthesis of synthetic hydrogels

The P[(HEMA<sub>0.85</sub>)-co-(MAA<sub>0.10</sub>)] hydrogels were molded on a silicon template of 6 mm diameter and 2 mm height by UV photopolymerization at 365 nm (4 mW/cm<sup>2</sup>) for 7 min. Previously, 70 µL Tri (ethylene glycol) dimethacrylate, as crosslinker, and 20 µL of Darocur, as initiator, were added to the ink.

#### B. Brillouin spectroscopy

Brillouin scattering measurements were performed with a virtually imaged phased array (VIPA)-based high-resolution optical Brillouin spectrometer as shown in Fig. 1. The setup consists of a commercially available inverted confocal microscope (IX81,

\*Contact author: pam@inst.org

†Contact author: mmm@inst.org

Olympus) coupled with a continuous-wave laser (532 nm, Cobolt Samba 100) and a 20 $\times$  (NA,0.42) objective as previously described [22]. Data analysis was carried out following the methods described in the reference papers [6,23].

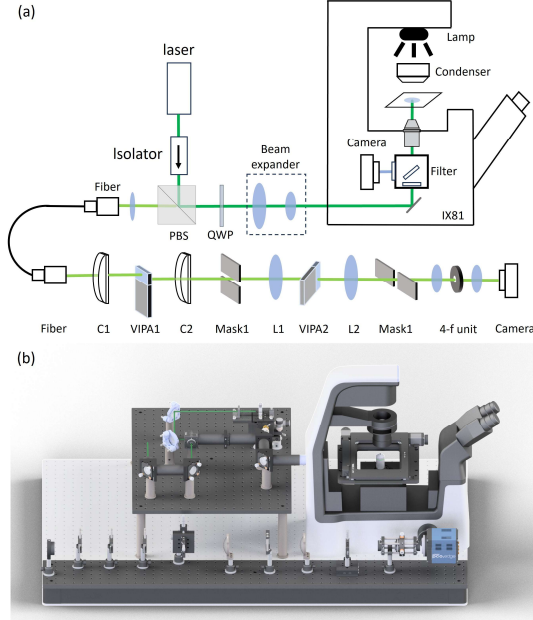


FIG 1. (a) Schematic of the Brillouin microscope setup. PBS, polarized beam splitter; QWP, quarter-wave plate; C1, C2, cylindrical lenses; VIPA1, VIPA2, virtually imaged phased array; L1, L2, lens while (b) is the corresponding 3D model.

### C. Rheology

The shear modulus ( $G$ ) was measured by a rheometer (Discovery Hybrid 20). An 8 mm diameter parallel-plate geometry was used for hydrogel samples, while liquid samples were measured using a 20 mm diameter, 0.5° cone-and-plate geometry. For hydrogels, measurements were performed within the linear viscoelastic regime using a frequency sweep from 0.1 to 5 Hz. The shear modulus was reported at 1 Hz and 1% strain at room temperature. For liquid samples, shear viscosity measurements were conducted over a frequency range from 1 to 30 kHz.

### IV. RESULTS

We first replicated previously reported hydrogel experiments which demonstrate a positive correlation between water content and elastic modulus [14]. In these experiments, the Brillouin shift indicates that the more water the hydrogel contains, the softer it becomes. In addition, within a certain range of water content, this relationship is approximately linear.

\*Contact author: pam@inst.org

†Contact author: mmm@inst.org

The representative Brillouin peaks for gelatin hydrogels of different concentrations are shown in the inset of Fig. 2(a), which indicates that the gels are homogeneous. As shown in Fig. 2(a), the Brillouin frequency shift ( $v_B$ ) and FWHM ( $\Gamma_B$ ) have a good linear correlation with water content. The values of  $v_B$  and  $\Gamma_B$  were obtained by fitting the spectra with a damped harmonic oscillator (DHO) model, in line with previous observations [14,24]. Based on the reference values for refractive index  $n$  and density  $\rho$  [14], we further derive the corresponding longitudinal storage modulus  $M'$  and loss elastic modulus  $M''$  in Fig. 2(b), by Eq. (2) and (3). Here  $\lambda$  is excitation wavelength (532 nm) and  $\theta$  is the collection angle of the scattered light, which is 180°.

Additionally, we measured shear modulus  $G$  of the same hydrogel using a rheometer at 1 Hz in Fig. 3. At low polymer concentrations, the shear modulus remains linearly correlated with the water content. Linear fits for loss modulus are provided for two distinct regimes, below 8% and above 8% polymer concentration. As the concentration increases beyond this threshold,  $G$  rises more sharply. This behavior reflects the polymer molecular arrangements in solutions. In dilute conditions, polymer chains exist as isolated coils, but at concentrations exceeding the coil overlap threshold, the chains begin to overlap and entangle, leading to a sharp increase in modulus.

This mechanical change was not captured in Brillouin scattering measurements. To illustrate this, we compared viscosity  $\eta$  obtained from both techniques. The loss modulus  $G''$  from rheometer is related to shear viscosity through  $\eta_s = G''/\omega$ , which refers to the dissipation of energy in viscous fluids. In the case of Brillouin shift, the longitudinal viscosity  $\eta_{long}$  can be estimated using Eq. (4) [13,14,16].

A comparison between the low-frequency shear viscosity measured with a Rheometer and the longitudinal viscosity inferred from Brillouin FWHM is shown in the inset of Fig. 3. Notably, the turning point at 8% polymer concentration indicates that the longitudinal viscosity is different from shear viscosity. Consistent with the findings of Wu et al., the Brillouin signal appears to be more influenced by water content than by the mechanical properties of the network [12]. This behavior can be understood by considering that the sensitivity of Brillouin microscopy to the solid polymer fraction vanishes in highly hydrated gels. Here, we aim to further clarify the origin of the

observed correlation between the Brillouin signal and water content.

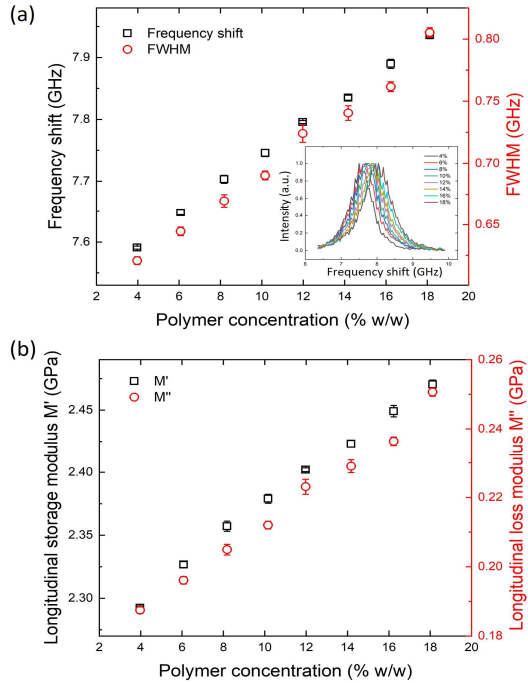


FIG 2. Gelatin hydrogels Brillouin spectroscopy. Dependence of (a) frequency shift and FWHM, the inset is normalized Brillouin anti-Stokes peak spectra; (b) storage and loss moduli via Brillouin spectra on polymer concentration.

As shown in Fig. 2, the Brillouin signal exhibits a strong linear correlation with the hydrogel's water content. This trend is intuitive that increasing water content generally leads to a softer hydrogel. Such linearity suggests that the water content can be estimated using a Voigt-type mixing model:

$$M_{\text{eff}} = (1 - x)M_1 + xM_{\text{water}} = (M_{\text{water}} - M_1)x + M_1, \quad (9)$$

where  $M_{\text{eff}}$  is the effective elastic modulus,  $M_1$  is the elastic modulus of hydrogel,  $M_{\text{water}}$  is the elastic modulus of water and  $x$  is the water content. Once  $M_1$  and  $M_{\text{water}}$  are calibrated, the water content can be estimated from this linear relationship. A similar result can be obtained if the material follows the Reuss model, which yields a weighted inverted average of the moduli. However, this apparent agreement does not imply that Brillouin measurements directly quantify water content. Correlation does not prove that there is a causal relationship. In fact, the correlation arises from the mixture's effective mechanical

response, not from a direct measurement of the water fraction itself.

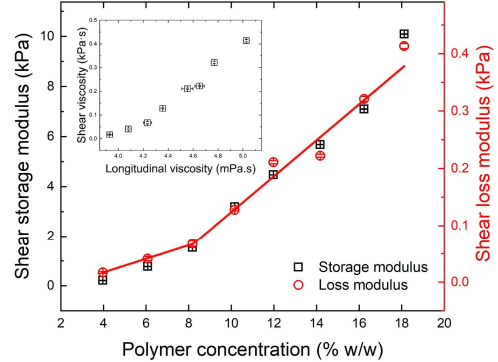


FIG 3. Storage and loss moduli via rheometer of gelation hydrogels on polymer concentration, the inset shows the relation between the low-frequency shear viscosity measured by rheometer and the high-frequency longitudinal viscosity inferred from the Brillouin FWHM.

To demonstrate this distinction, it is necessary to examine another gel system that behaves differently from porcine skin gelatin. In gelatin, the Brillouin shift closely follows hydration and approaches the value of pure water at high water content. This kind of behavior is often cited as evidence that Brillouin measurements primarily probe water concentration. To test the generality of this interpretation, we investigated a second hydrogel system,  $\text{P}[(\text{HEMA}_{0.85})\text{-co-(MAA}_{0.10}\text{)}]$ . In contrast to gelatin, chemical crosslinking in this network prevents the Brillouin shift from converging toward that of water upon hydration; instead, the shift increases, indicating hydration-induced stiffening.

Fig. 4 shows the hydration behavior of cylindrical hydrogel samples (6 mm in diameter and 2 mm in height) immersed in water. Brillouin microscopy measurements were performed at a depth of approximately 1 mm, and the results are presented in Fig. 4(a). Initially, since water requires some time to penetrate the interior of the hydrogel, the Brillouin shift and FWHM remain nearly constant. Once water reaches the probed region, both quantities increase rapidly. It is important to note that the Brillouin frequency of water is 7.5 GHz. After hydration, the sample's Brillouin frequency moves even farther from that of water rather than approaching it. This behavior reflects the BM shows hydration-induced changes in the network's mechanical properties during swelling instead of simple mixture models.

\*Contact author: pam@inst.org

†Contact author: mmm@inst.org

The corresponding shear moduli measured by rheometer are shown in Fig. 4(b). When probed as a whole, the cylindrical hydrogel samples exhibit changes that are slower than those captured by Brillouin microscopy. This contrast demonstrates that Brillouin microscopy is a powerful tool for resolving spatially localized mechanical changes within hydrogels during hydration. By measuring layer-specific responses at the microscale, it becomes possible to quantify how quickly different regions react upon water exposure. Ultimately, the overall elastic modulus of the hydrated hydrogel can be estimated by applying Voigt or Reuss effective-medium models. A detailed analysis of this approach will be presented in our future work, as it lies beyond the scope of the present study.

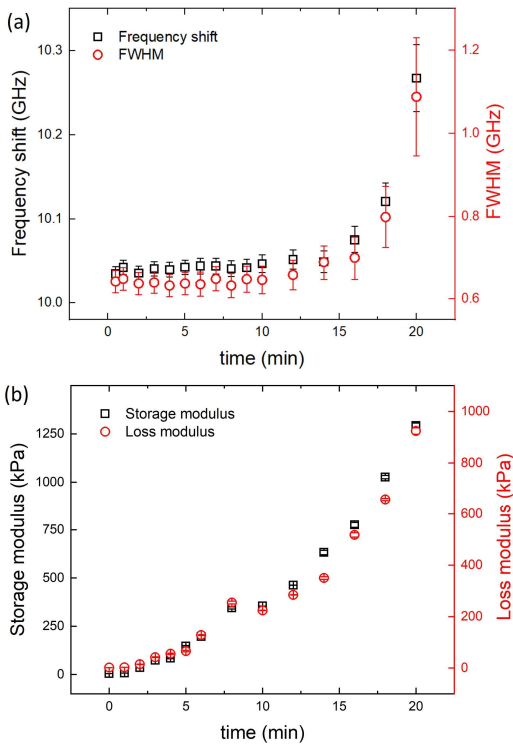


FIG 4. The hydration behavior of cylindrical P[(HEMA<sub>0.85</sub>)-co-(MAA<sub>0.10</sub>)] hydrogels samples; (a) Brillouin microscopy measurements, and (b) shear storage and loss moduli by rheometer of samples immersed in water as a function of time.

To further validate that Brillouin scattering reflects the mixture's effective mechanical response rather than directly measuring water fraction, we investigated ethanol–water mixtures, which is even simpler than hydrogels. Ethanol and water are both associating

\*Contact author: pam@inst.org

†Contact author: mmm@inst.org

liquids capable of hydrogen bonding and are miscible in all proportions. However, their longitudinal modulus and viscosity do not follow a simple linear mixing rule. These deviations arise because each component forms hydrogen-bonded networks with distinct microstructures. Individually, each liquid organizes to balance dense packing constraints with the formation of a preferred number of hydrogen bonds. Upon mixing, these competing structural tendencies interact, leading to non-ideal mechanical behavior [25].

A distinctive feature of ethanol–water mixtures is the existence of a maximum in sound velocity (proportional to FWHM) at approximately 66 vol% water at room temperature, as confirmed in Fig. 5(a). Consistent with this behavior, the Brillouin frequency shift also exhibits a maximum at intermediate compositions. In contrast, the linewidth reaches its maximum at a different composition, suggesting that the relaxation processes and elastic moduli respond differently to microstructures. Importantly, neither parameter varies monotonically with increasing water content, demonstrating that Brillouin scattering probes the mixture's complex mechanical response rather than simply tracking compositional changes.

To demonstrate that bulk viscosity is a non-negligible contribution, we compared the bulk and shear viscosities of ethanol–water mixtures. The shear viscosity shown in Fig. 5(b) was measured at 30 kHz. Additional measurements over the frequency range 1–30 kHz, presented in the Supplemental Material (SM), confirmed the expected frequency independence. The bulk viscosity was derived from the longitudinal and shear viscosity using Eq. (8). Densities of the mixed liquids were estimated using the Jouyban–Acree model, while refractive indices were obtained by interpolation from literature data [26,27]. All supporting data are provided in the SM. As shown in Fig. 5(b), the bulk viscosity is larger than the shear viscosity, indicating that this aspect of the mechanical response cannot be neglected, particularly in biomolecular systems.

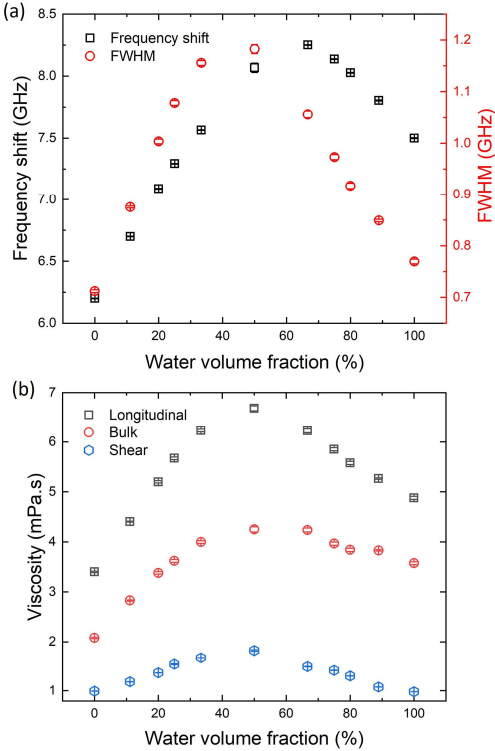


FIG 5. (a) Measured results of the Brillouin shift and the Brillouin linewidth in ethanol–water mixtures; (b) estimated longitudinal, bulk, and shear viscosities of the mixtures.

## V. CONCLUSIONS

Our findings demonstrated that Brillouin spectra are influenced but not directly measured hydration. By systematically tuning gelatin formulations and solvent compositions, we showed that Brillouin spectral

features can either positive or negative correlate with hydration, depending on the underlying mechanical response. Measurements on ethanol–water mixtures provide an independent and well-defined validation. It confirms that changes in Brillouin frequency shifts arise primarily from variations in mechanical properties rather than water content alone. Furthermore, by explicitly comparing longitudinal, bulk, and shear viscosities, we showed that the longitudinal response probed by Brillouin scattering incorporates significant contributions from bulk viscosity that are not captured by shear viscosity measurements alone. These results highlight the importance of considering the full viscoelastic response when interpreting Brillouin spectra in complex and biomolecular systems.

## ACKNOWLEDGMENTS

Z. W., R. M. and C. S. acknowledge the Funding from the European Research Council (ERC CoG no. 101001797 PHOTOMECH). F.T. and C.S. acknowledges support by the Deutsche Forschungsgemeinschaft (DFG; German Research Foundation) through SPP SE 1801/5-1 and the Volkswagenstiftung. A. G. and C. S. thank the European Research Council for funding through the Consolidator Grant NANOBEAT (no. 101177911). G. D. and C. S. would like to acknowledge funding by the DFG under Germany’s Excellence Strategy 2028/1-390761711 (3D Matter Made to Order), the Flagship Initiative “Engineering Molecular Systems.” And to the Carl Zeiss Foundation through the “Carl-Zeiss Foundation-Focus@HEiKA. We thank the Core Facility for the characterization of soft materials at IMSEAM of Heidelberg University.

- [1] K. H. Vining and D. J. Mooney, *Nature reviews Molecular cell biology* **18**, 728 (2017).
- [2] L. Vovard, A. Viel, E. Bastien, L.-A. Goutier, G. Jardine, J. Margueritat, S. Monnier, and T. Dehoux, arXiv preprint arXiv:2504.17362 (2025).
- [3] I. Kabakova, J. Zhang, Y. Xiang, S. Caponi, A. Bilenca, J. Guck, and G. Scarcelli, *Nature Reviews Methods Primers* **4**, 8 (2024).
- [4] A. B. Singaraju, D. Bahl, and L. L. Stevens, *AAPS PharmSciTech* **20**, 1 (2019).

- [5] K. V. Berghaus, S. H. Yun, and G. Scarcelli, *JoVE (Journal of Visualized Experiments)*, e53468 (2015).
- [6] J. Zhang and G. Scarcelli, *Nature protocols* **16**, 1251 (2021).
- [7] A. B. Roberts, J. Zhang, V. R. Singh, M. Nikolić, E. Moeendarbary, R. D. Kamm, P. T. So, and G. Scarcelli, *Journal of Biomechanics* **121**, 110400 (2021).
- [8] J. Margueritat *et al.*, *Physical review letters* **122**, 018101 (2019).
- [9] P. Shao, T. G. Seiler, A. M. Eltony, A. Ramier, S. J. Kwok, G. Scarcelli, R. Pineda II, and S.-H. Yun, *Investigative ophthalmology & visual science* **59**, 3020 (2018).

\*Contact author: pam@inst.org

†Contact author: mmm@inst.org

[10] C. Bevilacqua, H. Sánchez-Iranzo, D. Richter, A. Díz-Muñoz, and R. Prevedel, *Biomedical Optics Express* **10**, 1420 (2019).

[11] S. Mattana, S. Caponi, F. Tamagnini, D. Fioretto, and F. Palombo, *Journal of innovative optical health sciences* **10**, 1742001 (2017).

[12] P.-J. Wu, I. V. Kabakova, J. W. Ruberti, J. M. Sherwood, I. E. Dunlop, C. Paterson, P. Török, and D. R. Overby, *Nature methods* **15**, 561 (2018).

[13] S. Adichtchev, Y. A. Karpegin, K. Okotrub, M. Surovtseva, V. Zykova, and N. Surovtsev, *Physical review E* **99**, 062410 (2019).

[14] M. Bailey *et al.*, *Science advances* **6**, eabc1937 (2020).

[15] R. Rodríguez-López, Z. Wang, H. Oda, M. Erdi, P. Kofinas, G. Fytas, and G. Scarcelli, *Biomacromolecules* **25**, 955 (2023).

[16] J. Xu, X. Ren, W. Gong, R. Dai, and D. Liu, *Applied optics* **42**, 6704 (2003).

[17] C. Handler, G. Zanini, I. M. Smith, K. M. Stroka, G. Scarcelli, and C. Testi, *Communications Biology* **8**, 1645 (2025).

[18] A. S. Dukhin and P. J. Goetz, *The Journal of chemical physics* **130** (2009).

[19] S. Temkin and S. Temkin, *Elements of acoustics* (Wiley New York, 1981).

[20] H. Lamb, *Hydrodynamics* (University Press, 1924).

[21] G. Patterson and P. Carroll, *The Journal of Physical Chemistry* **89**, 1344 (1985).

[22] Z. Wang, Q. Jiang, C. Barwig, A. Mishra, K. Ramesh, and C. Selhuber-Unkel, *Journal of Physics: Photonics* (2024).

[23] P. Bouvet *et al.*, *Nature Photonics* **19**, 681 (2025).

[24] D. S. Bedborough and D. Jackson, *Polymer* **17**, 573 (1976).

[25] M. Mijaković, B. Kežić, L. Zoranić, F. Sokolić, A. Asenbaum, C. Pruner, E. Wilhelm, and A. Perera, *Journal of Molecular Liquids* **164**, 66 (2011).

[26] I. S. Khattab, F. Bandarkar, M. A. A. Fakhree, and A. Jouyban, *Korean Journal of Chemical Engineering* **29**, 812 (2012).

[27] R. Belda, J. Herraez, and O. Diez, *Physics and Chemistry of Liquids* **43**, 91 (2005).

\*Contact author: pam@inst.org

†Contact author: mmm@inst.org